Rapid Communications

Local probes for quantum Hall ferroelectrics and nematics

Pok Man Tam,[1,*] Tongtong Liu,[2,*] Inti Sodemann,[3] and Liang Fu[2]

[1]*Department of Physics and Astronomy, University of Pennsylvania, Philadelphia, Pennsylvania 19104, USA*
[2]*Department of Physics, Massachusetts Institute of Technology, Cambridge, Massachusetts 02139, USA*
[3]*Max-Planck Institute for the Physics of Complex Systems, D-01187 Dresden, Germany*

(Received 19 March 2020; revised manuscript received 19 May 2020; accepted 20 May 2020; published 3 June 2020)

Two-dimensional multivalley electronic systems in which the dispersion of individual pockets has low symmetry give rise to quantum Hall ferroelectric and nematic states in the presence of strong quantizing magnetic fields. We investigate the local signatures of these states arising near impurities that can be probed via scanning tunneling microscopy (STM) spectroscopy. For quantum Hall ferroelectrics, we demonstrate a direct relation between the dipole moment measured at impurity bound states and the ideal bulk dipole moment obtained from the modern theory of polarization. We also study the many-body problem with a single impurity via exact diagonalization and find that near strong impurities a nontrivial excitonic state can form with specific features that can be easily identified via STM spectroscopy.

DOI: 10.1103/PhysRevB.101.241103

Introduction. Recently, we have witnessed an explosion of high-quality two-dimensional electronic systems with strongly anisotropic dispersions that can be driven into the quantum Hall regime in the presence of strong magnetic fields [1,2], such as the (111) surface of bismuth [3–6], AlAs heterostructures [7,8], PbTe(111) quantum wells [9], and the (001) surface of a topological crystalline insulator (TCI) such as $Sn_{1-x}Pb_x(Te, Se)$ [10]. In these systems, at integer fillings of the Landau levels, the Coulomb interaction tends to spontaneously break symmetry by forming valley-polarized states [1,11–13], which can be generally divided into nematic or ferroelectric states according to whether or not the Fermi surface of an individual valley preserves inversion (or twofold rotation) symmetry [1]. Advances in scanning tunneling microscopy (STM) have made it possible to directly image the shape of Landau orbitals near impurities [3–5,14], providing an exciting window into these correlated states. Evidence of the quantum Hall ferroelectrics has been reported in bismuth (111) [4]. The surface of SnPb(Te,Se)-based TCIs is another promising platform to realize these states [15–19].

In this Rapid Communication we investigate the behavior of quantum Hall ferroelectrics and nematics near short-range impurities. One of our goals is to elaborate on how to measure an "order parameter" for the quantum Hall ferroelectricity. In trivial insulators in which the bulk and the boundary are simultaneously gapped, a natural order parameter is the ferroelectric dipole moment, which can be computed from the Berry-phase-based approach in the modern theory of polarization [20,21]. In quantum Hall ferroelectrics, although such polarization is well defined in an ideal setting subjected to periodic boundary conditions, it is unclear how to directly measure it due to screening at metallic boundaries. This issue can be resolved by studying states bound to impurities. Indeed, the ideal dipole moment defined by the modern theory of polarization can be related to that of impurity bound states, as we will demonstrate for the case of tilted Dirac cones relevant for the surface of SnPb(Te,Se)-based TCIs.

We also study numerically the many-body problem of states near short-range impurities by exact diagonalization. As previously discussed [3,4], the impurities can shift the energy of the occupied state that has a finite amplitude at the impurity location. We have found an interesting many-body regime where the impurity potential exceeds the exchange energy that attempts to keep the Landau level (LL) completely filled. For repulsive short-range impurities, once the impurity potential overcomes this threshold, a state with a quasihole bound to the impurity becomes the ground state of the system, and one of the lowest-lying excited states corresponds to a nontrivial intervalley excitonic state, in which an electron is added to another valley. We will discuss how these many-body states have clear signatures in STM measurements.

Impurity states for Dirac cones. Here, we consider a model that is relevant to the (001) surface of SnPb(Te,Se)-based TCIs. In these materials, at temperatures below a ferroelectric transition their surface states comprise four Dirac cones, two of which are massive and two massless. Each of the massive/massless pair is degenerate in the presence of time-reversal symmetry [19], but under a background magnetic field the degeneracy of the massive pair is no longer protected. The degeneracy of the massless pair will however remain protected by the product of time reversal and a mirror symmetry (see Supplemental Material [22]). Here, we focus on the latter two degenerate valleys. The dispersions generally have a tilt in momentum [17,23], which is essential to the ferroelectricity that we describe below. We thus consider the following effective Hamiltonian for the Dirac cone at $\pm\bar{\Lambda}$ (near $\bar{X}$),

$$H = v_x\sigma_x p_x - v_y\sigma_y p_y \pm \delta v_x p_x + \Delta\sigma_z, \tag{1}$$

[*]These authors contributed equally to this work.

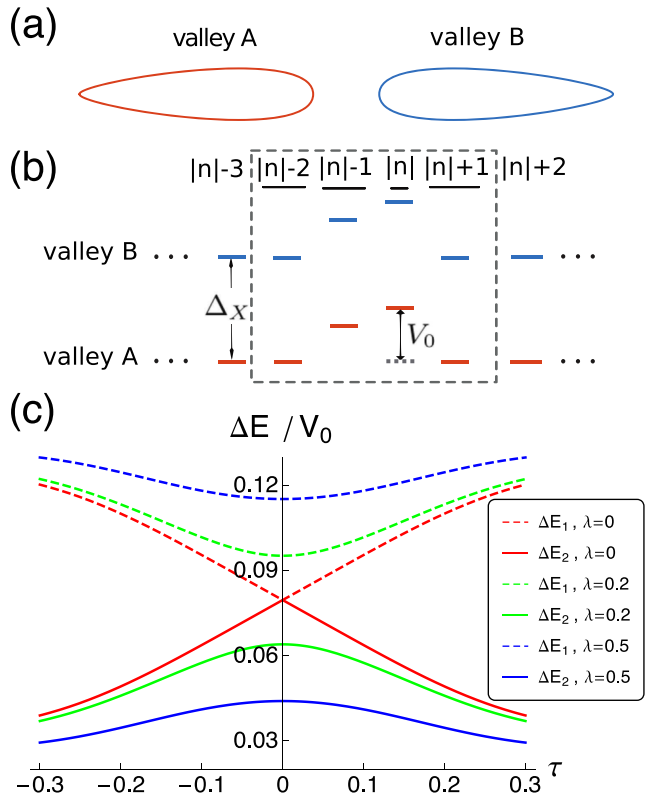

FIG. 1. (a) Simplistic illustration of a quantum Hall ferroelectric system. The Fermi surface consists of two valleys related by a twofold rotation, while an individual valley breaks (preserves) twofold rotation symmetry for the ferroelectric (nematic) state. (b) Schematic of single orbit spectra, for the nth Dirac Landau level: Upon hybridization only two states are perturbed in energy by a delta-function impurity V_0 [22]. The exchange splitting Δ_X favors valley polarization. (c) Energies ΔE_1 and ΔE_2 of the two impurity states for the $n = \pm 1$ Dirac Landau level, as a function of the tilt (τ) and mass (λ) of the Dirac cone.

where σ_i are Pauli matrices and δv_x represents the tilt of the Dirac cone. For generality we have added a mass term $\Delta\sigma_z$ to the originally massless Dirac cones which is allowed in magnetic fields due to the Zeeman effect, however, in TCIs this coupling has been seen to be negligibly small [10]. In the presence of external magnetic fields Landau levels will form, and we consider a partial filling $\nu = 1$ for the resulting twofold degenerate valley doublet. The quantum Hall ferroelectric (nematic) state forms when the electrons spontaneously polarize into a single one of these valleys due to interactions [1]. Figures 1(a) and 1(b) provide simplistic illustrations of this model. Inspired by recent STM experiments [3,4], we study states near short-range impurities modeled as delta-function potentials [24],

$$H_{\text{imp}} = V_0 l_B^2 \, \delta(\mathbf{r}), \tag{2}$$

where $l_B = \sqrt{\hbar c/eB}$ is the magnetic length. Assuming that the impurity potential (V_0) is smaller than the Landau level spacing, we project the Hamiltonian to the Landau level of interest. Only states with a finite probability at the origin will be affected by the impurity potential. For a parabolic

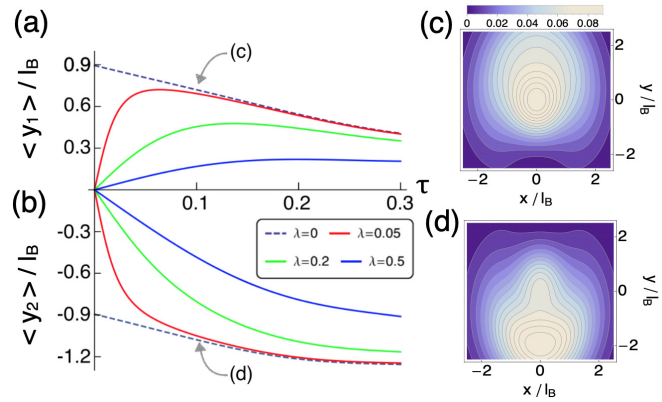

FIG. 2. (a), (b) Average position, measured from the impurity site, of the impurity states from the $n = -1$ Dirac LL, as a function of the tilt (τ) and mass (λ) of the Dirac cone. (c), (d) Spatial probability distribution of the impurity states (for TCI parameters $\tau = 0.1$, $\lambda = 0$, and $v_x/v_y = 1.6$), which can be probed by the tunneling differential conductance in STM.

dispersion, there would be a single state per Landau level with nonzero probability at the origin, as demonstrated in the bismuth experiments [3]. However, the situation is richer for Dirac Landau levels due to the two-component nature. Some distinctions between the conventional and Dirac Landau levels have been revealed in STM experiments on the surface of topological insulators [25], and here we discuss another distinction regarding the impurity state. The wave function of the nth Dirac Landau level in the massless and untilted limit (for the general case, see the Supplemental Material [22]) is

$$\psi_{n,m} = \frac{1}{\sqrt{Z_n}} \begin{pmatrix} \phi_{|n|,m} \\ s_n \phi_{|n|-1,m} \end{pmatrix}, \tag{3}$$

where $n \in \mathbb{Z}$, $s_n = \text{sgn}(n)$ (with $s_0 = 0$), $Z_n = 2^{|s_n|}$, and $\phi_{|n|,m}$ is the wave function for a parabolic Landau level in the symmetric gauge with angular momentum $m - |n|$. For the $n = 0$ LL only the $m = 0$ state would have probability at the origin, however, for $n \neq 0$, two states with $m = |n|$ and $m = |n| - 1$ would have probability at the origin and opposite pseudospins [26,27]. These two states are exactly degenerate for a massless and untilted dispersion, but either of these perturbations produces an energy splitting as illustrated in Fig. 1. Thus the impurity states are generically resolvable in STM measurements. In the Supplemental Material [22] we demonstrate that these perturbations do not produce extra impurity states, and therefore only these two states are split from the bulk Landau level and bound to the impurity. Let us introduce dimensionless parameters to characterize the tilt $\tau \equiv \delta v_x/(2v_x)$ and the mass $\lambda \equiv \Delta l_B/(\sqrt{2v_x v_y})$. In $Sn_{1-x}Pb_x(Te, Se)$ these are approximately $\tau = 0.1$, $\lambda = 0$ (neglecting Zeeman effect), and $v_x/v_y = 1.6$ [22]. It is therefore justified to use perturbation theory in τ. The splitting of the two impurity states from the bulk $n = \pm 1$ Landau level, to leading order in τ, are then estimated to be $\Delta E_1 \approx 0.10V_0$, $\Delta E_2 \approx 0.06V_0$. Figure 2 displays the spatial profile of these two states.

Ferroelectric dipole moments. In the modern theory of electric polarization [20,21], the dipole moment of an insulator

is computed by adopting periodic boundary conditions. The dipole is computed from the change of the electronic position while varying the Hamiltonian along an adiabatic path in which the bulk gap remains open and that starts from an inversion symmetric reference state. Following this principle a dipole moment for the ferroelectric quantum Hall state was introduced in Ref. [1]. For tilted Dirac cones, this dipole moment per particle to leading order in the tilt is

$$\mathbf{D}_n = \tilde{s}_n \sqrt{2}\, \tau\, e\, l_B \left(\frac{2\lambda^2 + 3|n|}{\sqrt{\lambda^2 + |n|}} \right) \sqrt{\frac{v_y}{v_x}}\, \hat{\mathbf{y}}, \tag{4}$$

where $\tilde{s}_n = \mathrm{sgn}(n)$ (with $\tilde{s}_0 = 1$). Notice that the dipole along the tilt (x axis) vanishes [1]. The limitation of this definition is that one assumes the charge that flows through the bulk will appear intact at the surface, providing a net electric polarization. However, in an insulating topological phase with a metallic boundary, the latter assumption is unjustified since the surface charge can flow and lead to vanishing macroscopic polarization. Hence it is important to devise alternative diagnostics of the inversion asymmetry in topological phases such as the quantum Hall ferroelectrics.

Impurity states, which can be locally probed by STM, offer a resolution. For any given impurity state one can define a dipole moment as the expectation value of the position measured relative to the center of the impurity potential. If the impurity potential is inversion symmetric, this dipole moment serves to characterize the inversion asymmetry of the host state. Figures 2(a) and 2(b) display the average position of the impurity states in tilted Dirac cones as a function of their mass and tilt. Interestingly, the average position is nonanalytic, as evidenced by the fact that the limits of $\tau \to 0$, $\lambda \to 0$ do not commute in Fig. 2. This is a consequence of the fact that in this limit both impurity states are degenerate and hence the expectation values on individual states become ambiguous. However, the sum of the average positions in both impurity states is free from ambiguities and vanishes as $\tau \to 0$, $\lambda \to 0$. We therefore introduce the notion of the *impurity dipole moment* $\mathbf{D}^{\mathrm{imp}}$ as the sum of the average position of impurity states ψ_i,[1]

$$\mathbf{D}^{\mathrm{imp}} = e \sum_i \langle \psi_i | \mathbf{r} | \psi_i \rangle. \tag{5}$$

To leading order in the tilt (τ) and mass (λ) of the Dirac cone, we obtained the following relation between the adiabatic bulk dipole moment, in Eq. (4), and the impurity dipole moment,

$$\mathbf{D}_n^{\mathrm{imp}} = \frac{2|n|}{3|n| + 2\lambda^2} \mathbf{D}_n, \tag{6}$$

for the nth Dirac Landau level in a Dirac cone of mass λ (the derivation is presented in the Supplemental Material [22]). This formula summarizes one of the key messages of our study: Local measurement of the impurity dipole moment $\mathbf{D}^{\mathrm{imp}}$, combined with the knowledge of the electronic structure, can be used to probe the bulk adiabatic dipole moment following from the modern theory of polarization $\mathbf{D}$ in a quantum Hall ferroelectric state.

In the massless limit, i.e., $\lambda \ll \sqrt{|n|}$, the two dipole moments have a simple proportionality relation, $\mathbf{D}_n^{\mathrm{imp}} = (2/3)\mathbf{D}_n$. However, a notable difference between these two notions appears in the large mass limit, i.e., $\lambda \gg \sqrt{|n|}$, for which the adiabatic dipole grows linearly with the mass, $|\mathbf{D}_n| \propto \lambda$, whereas $|\mathbf{D}_n^{\mathrm{imp}}| \propto 1/\lambda$. This markedly different behavior is a consequence of the approach to the parabolic mass limit as we explain in the Supplemental Material [22].

Many-body physics near impurities. So far we have largely ignored the role of electron-electron interactions by imagining that a large self-consistent exchange field has set in to select a single valley. Next, we will study the many-body problem in the presence of the impurity potential from Eq. (2) by means of exact diagonalization on a torus. We concentrate here on the ferroelectric states where two valleys are described by the tilted massless Dirac cone with the same axis orientation and velocity ratio but opposite tilt. We expect the states at the Landau level $n = +3$ to essentially carry over to the case of bismuth surfaces [3–6]. In the Supplemental Material [22], we also present a nematic model of two valleys with anisotropic masses whose principal axes are rotated by $\pi/2$, as in AlAs quantum wells [7,8], which gives a simpler picture of what we find.

In the absence of impurity ($V_0 = 0$) at the $n = +3$ Dirac LL and partial filling $\nu = 1$, the ground state of the system spontaneously polarizes into a single valley and an exchange splitting Δ_X between the two valleys develops [1,12,13]. This is schematically depicted in Figs. 1(a) and 1(b). In the forthcoming discussion we choose the chemical potential to lie exactly in the middle of the charge gap, namely, we add a single particle term to the Hamiltonian so that far away from the impurity the energy to add one electron equals the energy to add one hole. In STM spectra this is satisfied when the two peaks corresponding to the occupied and empty valleys in the Landau level are located symmetrically away from zero bias with no impurity, as illustrated in Fig. 3. We assume a sufficiently strong tilt so that the lowest-energy charged excitations are not skyrmions [1].

We denote the valley polarization of states by a vector $(N_{\mathrm{A}}, N_{\mathrm{B}})$, where N_i is the number of electrons in valley i ($i = \mathrm{A}, \mathrm{B}$). The ground state at $\nu = 1$ in the absence of the impurity therefore has polarization $(N_\phi, 0)$. The number of orbits in a single valley is taken to be $N_\phi = 40$. STM is customarily viewed as a probe of the density of states of the single particle charged excitations, because it requires the removal or injection of electrons from the sample. As we will see, however, near strong impurities, it is possible to use STM to probe excitonic states. For a weak impurity, $V_0 \ll \Delta_X$, as the STM tip is brought near the impurity one expects simply a shift of the spectrum by an energy $\sim V_0$, reflecting the local change of energy to remove/add particles as illustrated by peaks A, B in Fig. 3. In this regime one encounters excitonic states inside the gap. However, they are *invisible* in the STM spectrum because they are *neutral* and hence orthogonal to states with added/removed electrons relative to the ground state.

[1]This average coincides with the minus of the dipole moment weighted by the charge distribution of the hole that is left in the Landau level which can also be directly accessed by STM measurements.

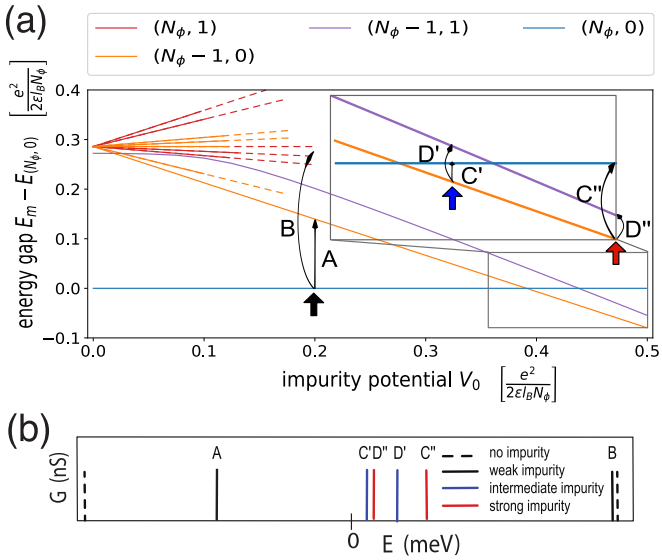

FIG. 3. (a) Spectra with increasing impurity potential: (N_A, N_B) labels the state with N_A electrons in valley A and N_B electrons in valley B. Energy is measured relative to that of $(N_\phi, 0)$. Notice that the ground state is changed from $(N_\phi, 0)$ to $(N_\phi - 1, 0)$ as the repulsive impurity becomes stronger. Here, we use $N_\phi = 40$, $\tau = 0.1$, $v_x/v_y = 5$, and $\lambda = 0$. (b) Illustration of tunneling peaks measured via STM. The peaks are labeled in correspondence with tunneling processes indicated in the upper panel. For simplicity in (b) we only show one of the two impurity levels that split from the bulk Landau level. The other is visible in (a) as a solid-dashed orange line.

Interestingly, when the impurity potential exceeds a threshold on the order of exchange splitting, the ground state of the system is no longer the fully valley-polarized state $(N_\phi, 0)$ but rather a quasihole state with polarization $(N_\phi - 1, 0)$,[2] as described in Fig. 3(a). This is essentially a local doping of the ground state by removing one electron. Importantly, there appear then two energetically close excited states with quantum numbers $(N_\phi, 0)$ and $(N_\phi - 1, 1)$. These two lowest excited states differ from the ground state by *adding* a single electron, and hence will appear as two peaks (C and D) at positive bias in the STM spectrum, as shown in Fig. 3(b). These two peaks shift sides as V_0 increases, when the energy of $(N_\phi, 0)$ exceeds $(N_\phi - 1, 1)$. Experimentally these peaks can be distinguished by probing the respective spatial differential conductance, as detailed in Fig. 4.

The $(N_\phi - 1, 1)$ state can be viewed as an excitonic state bound to the impurity. Since it differs from the local ground state by one electron, its wave function can be imaged by STM. The differential conductance of adding an electron in STM is given by the local density of states (LDOS) at

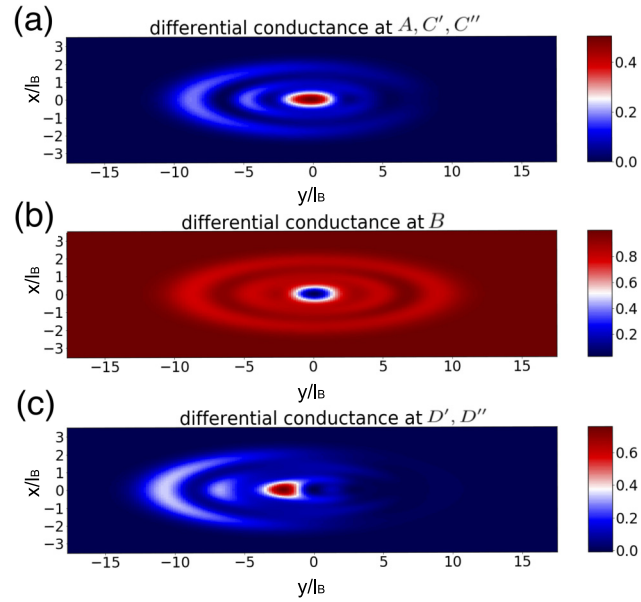

FIG. 4. The local density of states at energy levels A, B, C', D', C'', D'', which is proportional to the differential conductance obtained by STM measurements. The unit of length is set to be l_B. The tilt $\tau = 0.1$ and velocity ratio $v_x/v_y = 5$ are used.

energy ε,

$$G(\mathbf{r}) \propto \sum_m \left| \langle \phi_m | \sum_j [c^\dagger_{A,j} \phi^*_{A,j}(\mathbf{r}) + c^\dagger_{B,j} \phi^*_{B,j}(\mathbf{r})] | \phi_0 \rangle \right|^2, \quad (7)$$

where $|\phi_0\rangle$ is the lowest-energy state. For a weak impurity below the threshold, $|\phi_0\rangle = |N_\phi, 0\rangle$. Above the threshold, $|\phi_0\rangle = |N_\phi - 1, 0\rangle$, which is the hole state created by the impurity. $c^\dagger_{i,j}$ and $\phi_{i,j}$ are the creation operator and single electron wave function for an orbit j on valley i. $\langle \phi_m |$ is the state with energy ε, and the sum over m is taken for all degeneracy. The case of removing an electron follows from Eq. (7) by replacing $c^\dagger_{i,j}$ and $\phi^*_{i,j}$ with $c_{i,j}$ and $\phi_{i,j}$, respectively.

Figure 4 depicts the expected shape of the differential conductance in STM at the energy and impurity indicated in Fig. 3. The B peak in the spectroscopy includes multiple nearly degenerate states, and here in Fig. 4 we treat them as degenerate at energy ε and average over them. The first two panels of Fig. 4 depict tunneling between a single-hole or electron state and the fully polarized state, which only involves single-body physics; while the last panel is the tunneling between the hole state and the excitonic state, though only reflecting the LDOS of valley B with one electron, its shape is modified via the interaction with the hole in valley A. The significant difference between Figs. 4(a) and 4(c) allows for distinguishing this nontrivial excitonic state in STM.

Summary. We have studied how to locally probe quantum Hall ferroelectric and nematic states near short-range impurities. Particularly the impurity dipole moment, which is measurable via STM, is introduced to characterize the degree of inversion asymmetry in quantum Hall ferroelectrics. We have also investigated the many-body problem near strong impurities and found nontrivial excitonic states. These states, though typically invisible in STM near weak impurities,

[2]Here, we describe the behavior for repulsive impurities $V_0 > 0$, but equivalent statements hold for attractive impurities after performing a particle-hole conjugation $(N_A, N_B) \to (N_\phi - N_B, N_\phi - N_A)$. Particularly, the quasihole state in the repulsive case is replaced by a quasiparticle state in the attractive case.

become accessible near strong impurities which change the ground state by locally removing/adding an electron.

Acknowledgments. We are grateful to Benjamin Feldman, Mallika Randeria, and Ali Yazdani for illuminating discussions. T.L. would like to thank Zheng Zhu for helping with the numerical study. This work is supported by DOE Office of Basic Energy Sciences under Award No. DE-SC0018945. P.M.T. was in part supported by the Croucher Scholarship for Doctoral Study from the Croucher Foundation.

[1] I. Sodemann, Z. Zhu, and L. Fu, Phys. Rev. X **7**, 041068 (2017).
[2] S. A. Parameswaran and B. E. Feldman, J. Phys.: Condens. Matter **31**, 273001 (2019).
[3] B. E. Feldman, M. T. Randeria, A. Gyenis, F. Wu, H. Ji, R. J. Cava, A. H. MacDonald, and A. Yazdani, Science **354**, 316 (2016).
[4] M. T. Randeria, B. E. Feldman, F. Wu, H. Ding, A. Gyenis, H. Ji, R. J. Cava, A. H. MacDonald, and A. Yazdani, Nat. Phys. **14**, 796 (2018).
[5] M. T. Randeria, K. Agarwal, B. E. Feldman, H. Ding, H. Ji, R. J. Cava, S. L. Sondhi, S. A. Parameswaran, and A. Yazdani, Nature (London) **566**, 363 (2019).
[6] K. Agarwal, M. T. Randeria, A. Yazdani, S. L. Sondhi, and S. A. Parameswaran, Phys. Rev. B **100**, 165103 (2019).
[7] M. Shayegan, E. P. De Poortere, O. Gunawan, Y. P. Shkolnikov, E. Tutuc, and K. Vakili, Phys. Status Solidi B **243**, 3629 (2006).
[8] T. Gokmen, M. Padmanabhan, and M. Shayegan, Nat. Phys. **6**, 621 (2010).
[9] V. A. Chitta, W. Desrat, D. K. Maude, B. A. Piot, N. F. Oliveira, Jr., P. H. O. Rappl, A. Y. Ueta, and E. Abramof, Physica E **34**, 124 (2006).
[10] Y. Okada, M. Serbyn, H. Lin, D. Walkup, W. Zhou, C. Dhital, M. Neupane, S. Xu, Y. J. Wang, R. Sankar, F. Chou, A. Bansil, M. Z. Hasan, S. D. Wilson, L. Fu, and V. Madhavan, Science **341**, 1496 (2013).
[11] X. Li, F. Zhang, and A. H. MacDonald, Phys. Rev. Lett. **116**, 026803 (2016).
[12] D. A. Abanin, S. A. Parameswaran, S. A. Kivelson, and S. L. Sondhi, Phys. Rev. B **82**, 035428 (2010).
[13] A. Kumar, S. A. Parameswaran, and S. L. Sondhi, Phys. Rev. B **88**, 045133 (2013).
[14] Z. Papić, R. S. K. Mong, A. Yazdani, and M. P. Zaletel, Phys. Rev. X **8**, 011037 (2018).
[15] P. Dziawa, B. J. Kowalski, K. Dybko, R. Buczko, A. Szczerbakow, M. Szot, E. Lusakowska, T. Balasubramanian, B. M. Wojek, M. H. Berntsen, O. Tjernberg, and T. Story, Nat. Mater. **11**, 1023 (2012).
[16] T. H. Hsieh, H. Lin, J. Liu, W. Duan, A. Bansil, and L. Fu, Nat. Commun. **3**, 982 (2012).
[17] Y. Tanaka, Z. Ren, T. Sato, K. Nakayama, S. Souma, T. Takahashi, K. Segawa, and Y. Ando, Nat. Phys. **8**, 800 (2012).
[18] J. Liu, W. Duan, and L. Fu, Phys. Rev. B **88**, 241303(R) (2013).
[19] M. Serbyn and L. Fu, Phys. Rev. B **90**, 035402 (2014).
[20] D. J. Thouless, Phys. Rev. B **27**, 6083 (1983).
[21] R. D. King-Smith and D. Vanderbilt, Phys. Rev. B **47**, 1651(R) (1993).
[22] See Supplemental Material at http://link.aps.org/supplemental/10.1103/PhysRevB.101.241103 for more details about the setup of our theoretical and numerical studies.
[23] I. Sodemann and L. Fu, Phys. Rev. Lett. **115**, 216806 (2015).
[24] For simplicity we neglect intervalley scattering although it has been recently shown that certain detailed aspects of the states near the impurity require understanding the intervalley scattering properties [4].
[25] Y.-S. Fu, M. Kawamura, K. Igarashi, H. Takagi, T. Hannaguri, and T. Sasagawa, Nat. Phys. **10**, 815 (2014).
[26] A. H. MacDonald, *Introduction to the Physics of the Quantum Hall Regime*, Proceedings of the 1994 Les Houches Summer School on Mesoscopic Physics (Elsevier, Amsterdam, 1995).
[27] G. Giuliani and G. Vignale, in *Quantum Theory of the Electron Liquid* (Cambridge University Press, Cambridge, UK, 2008), p. 559.